FINITE ELEMENT SIMULATION OF CRACK PROPAGATION IN MILITARY AIRCRAFT COATINGS

Bing Han[a], Martin Veidt[b], Donna Capararo[c], Graeme George[d]
[a,b,d]Mechanical & Mining School, University of Queensland, St Lucia, QLD 4072, Australia
[c]AIBN, University of Queensland, St Lucia, QLD 4072, Australia
[a,c,d]Defence Materials Technology Centre, Hawthorn, VIC3122, Australia
[a]*bing.han1@uqconnect.edu.au*; [b]*m.veidt@uq.edu.au*; [c]*uqdcapar@uq.edu.au*,
[d]*g.george@uq.edu.au*

Keywords: *aircraft coating, paint degradation, crack growth, A-FEM, CZM*

Abstract

Environmental degradation is a major problem that decreases durability of military aircraft coatings. Micro-cracks may form and propagate during service and environmental exposure. This paper reports on the development and validation of a special purposed finite element program that can predict micro-crack evolution in aircraft coatings.

1 Introduction

Corrosion is one of the main maintenance cost drivers for military aircraft. A United States National Research Council report [1] stated that corrosion costs the USAF approximately US$1 billion annually.

Typical aircraft coatings consist of two layers – polyurethane (PU) topcoat and epoxy primer (*Figure 1*). They are applied on the metal substrate as the primary protection against metal corrosion. During flight the coating must withstand flexural movement. Fresh coating has rather good flexibility to cope with the bending load. However, as it is exposed to environmental factors such as UV radiation, water, temperature fluctuation and so on, its properties start to degrade and it becomes more brittle. Micro-cracks may form and grow in coatings under mechanical loading. Those cracks can allow moisture to come into contact with the substrate and subsequently initiate corrosion (*Figure 2*). As noted by Clark [2], the prediction of overall service life of a corroded part is critically sensitive to the coating life, and improved coating durability is a key goal in managing that overall life.

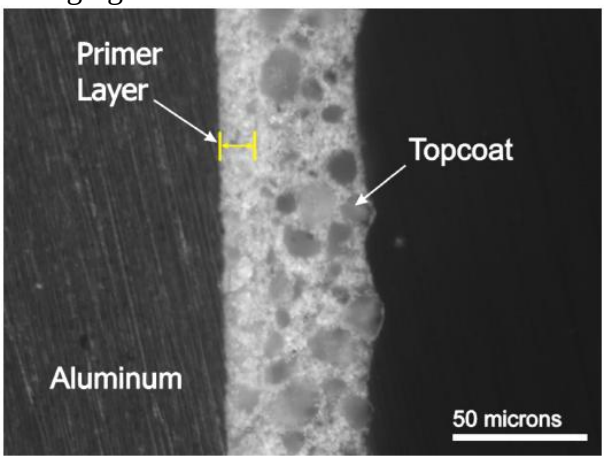

Figure 1 Typical aircraft coatings [3]

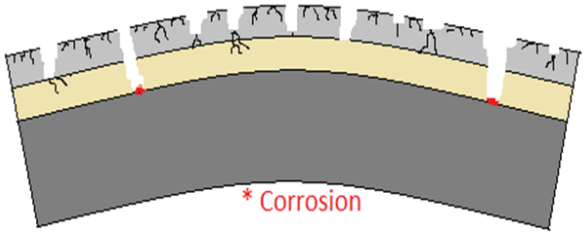

Figure 2 Coating cracking after degradation

Substantial experimental work exists on the degradation of aircraft coatings. However, numerical studies of crack behavior during aircraft coating degradation do currently not exist. This paper reports on the development and validation of a special purpose finite

element (FE) program that can predict micro-crack evolution in aircraft coatings.

This paper is organized as follows: Section 2 reviews background literature on crack growth modeling. Section 3 presents A-FEM formulation used in this paper for crack growth simulation. Section 4 uses two numerical examples to demonstrate the validity of the developed program. Section 5 demonstrates and discusses results of aircraft coating studies. Finally, Section 6 provides summaries and conclusions.

2 Literature review

Engineering problems requiring crack growth analysis have received increased attention in recent years. The direct way to study crack behavior numerically is to use fracture mechanics in conjunction with the FE method. Linear elastic fracture mechanics (LEFM) has been developed and implemented within commercial FE codes to study a variety of fracture problems. For example, stress intensity factor (SIF) or strain energy release rate can be calculated based on displacement field obtained from FE analysis. Essential to the success of LEFM approaches is the requirement of a small process zone ahead of the crack tip [4]. Therefore, LEFM is applicable to brittle or quasi-brittle material with small scale plasticity. When the process zone is larger than the characteristic length scale in the problem, elastic-plastic fracture mechanics (EPFM) applies. The J-integral elastic plastic fracture criterion based on the path independent energy line developed by Rice [5], enables to predict fracture in structures in cases of both large as well as small-scale plasticity. The fracture criteria mentioned above provide one parameter failure criteria for those cracked bodies and are valid for the analysis of stationary cracks. When applying to growing cracks, remeshing is required. This approach suffers from the major disadvantage of low efficiency, because remeshing is required for every incremental step of crack growth.

An alternative approach to the singularity driven fracture methods discussed above is the cohesive zone model (CZM) approach proposed by Dugdale [6] and Barenblatt [7] for elastic-plastic fracture in ductile metals. Hillerborg et al [8] introduced the concept of fracture energy into the cohesive crack model and extended its application to quasi-brittle materials. In the CZM, a narrow-band zone is assumed to exist ahead of a crack tip which represents the fracture process zone. So-called cohesive tractions act on the cohesive surfaces. A cohesive constitutive law relates the cohesive traction to the opening displacement of the cohesive surfaces. Compared to conventional fracture mechanics, CZM utilizes a complete traction-separation law to describe a fracture process, rather than a single energy based parameter. This makes CZM very adaptive to any particular fracture process: simply by varying the cohesive law different fracture processes can be represented without changing any numerical aspect of the CZM. CZM not only avoids the singularity at crack tip but also can be easily implemented in a numerical method as in FEM. By inserting cohesive zone interface elements between continuum elements along the potential crack path, a cohesive crack can be modeled without remeshing. However, one shortcoming associated with the use of CZM is that the potential crack path needs to be known before crack growth, so that CZM elements can be directly introduced along the path. This greatly limits the application of CZM for problems with evolving arbitrary cracks.

The numerical methods mentioned above require the finite element edges to coincide with the crack. An extension of FEM called the extended finite element method (X-FEM) has been developed by Belytschko et al. [9, 10] to model arbitrary discontinuities independently of the finite element mesh. This flexibility enables the method to simulate crack growth without remeshing. At first, the crack surfaces were considered free of tractions in X-FEM. Then Dolbow et al. [11] incorporated contact and friction on the crack faces to simulate crack growth under compression. Later Belytschko and Moës [12] integrated CZM into the X-FEM framework to overcome the CZM shortcoming because the X-FEM is particularly effective in dealing with moving arbitrary discontinuities.

The key feature in X-FEM formulation is the use of enrichment functions for cracked elements locally. This is achieved by enhancing DoFs of all the nodes employed by the elements with internal discontinuity. The need of remeshing when a crack advances is eliminated by introducing local enrichment to the cracked elements. X-FEM approach has now been widely used in arbitrary cracking analyses of many engineering materials including composite materials [13-15]. Nevertheless, X-FEM also has its drawbacks. First, the crack-tip singular displacement fields and free displacement functions have to be known a priori, so that they can be incorporated into X-FEM as enrichment functions. In highly heterogeneous material such as composites different cracking systems often interact with each other. For example, a splitting crack interacts with a delamination crack. At the joint front when the two cracks interact directly, no known solution exists. X-FEM will have difficulty in dealing with this type of problems. Another inconvenience of X-FEM in dealing with arbitrary cracking problems is that it enriches elemental displacement field through adding nodal DoFs, which requires dynamic adjustment of nodal DoFs according to whether a node is completely cut or not. This leads to not only algorithmic changes of standard FEM, but also incompatibility of X-FEM elements and traditional elements [16, 17].

A promising alternative numerical method for handling arbitrary cracking problems is the augmented finite element method (A-FEM). This line of development follows the original work of Hansbo & Hansbo [18, 19], who first established that an arbitrary discontinuity within an element can be introduced by adding an extra element on top of the existing element, with each element accounting for the stiffness and force contribution from the bisected physical domains. The addition of elements is typically realized by introducing additional nodes that are geometrically identical to the original corner nodes. Hence this method is also named phantom node method [20-22]. The formulation is different from X-FEM but it has been shown by Areias & Belytschko [23] that they are equivalent – the basic functions in Hansbo & Hansbo's element are simply a linear combination of the X-FEM basic functions. More recently, Steinmann and colleagues [24-27] have coupled Hansbo & Hansbo's method with CZMs to cope with arbitrary fracture problems in homogeneous, isotropic materials. The name of A-FEM was coined by Ling & Yang [16], who applied this method to composite materials with high heterogeneity. One major advantage of this method is that it uses only standard FE shape functions and thus avoids the use of enrichment functions as in X-FEM. It fully preserves elemental locality and hence can be made compatible with commercial FEM programs. The proposed formulation enables the use of standard finite element shape functions without any truncation across the discontinuity, which greatly facilitates the use of the augmented elements in conjunction with CZM.

Because of these advantages, A-FEM was selected in this project as the numerical tool for modeling crack evolution behavior in the polymer matrix. CZM method was used to study crack behavior at material interfaces by inserting interface elements along filler boundaries and the topcoat-primer interface. Therefore, the whole crack evolution behavior can be investigated by combining A-FEM and CZM methodologies. Since the CZM is a well known method in modeling crack growth, only the details of A-FEM formulation will be described in the following chapter.

3 A-FEM formulation and implementation

3.1 Element formulation

Consider an element in a finite element mesh with nodes 1-2-3-4 (see *Figure 3*a). This element is crossed by a cohesive crack at Γ_c, dividing the element domain Ω^e into two complementary sub-domains, Ω_1^e and Ω_2^e . The two severed physical domains can be separately approximated by two mathematical elements (MEs) as shown in *Figure 3b* and *c*. Both MEs have the identical geometry to the discontinuous physical element (PE) and use standard shape

functions for elemental displacement field interpolation, but with different material allocation. In ME1, which represents the physical response of Ω_1^e, the active material domain (shaded area) for stiffness and nodal force integration has the identical geometry of Ω_1^e, while the rest of the ME1 does not contribute to the stiffness of the element. Two additional nodes 3' and 4' are introduced to facilitate the elemental displacement interpolation and they share the same geometrical locations with the corresponding physical nodes (3 and 4). Similarly, ME2 represents the physics response of Ω_2^e with two added nodes 1' and 2'. These added nodes are named "phantom nodes". These phantom nodes are not shared by any neighboring elements other than those elements traversed by the same discontinuity. Therefore, each ME has independent displacement fields. The two mathematical elements are connected by a cohesive traction along the crack line.

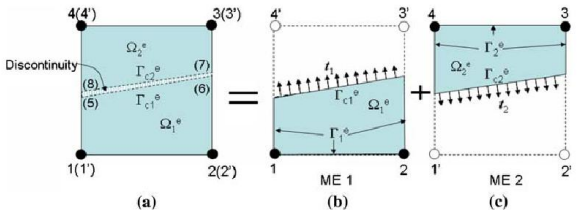

Figure 3 An element traversed by an intra-element cohesive crack (a). This element can be treated by defining two mathematical elements (b and c), each has the same geometrical dimension as the original but with different physical material domains for stiffness integration[16]

The finite element equations for the MEs can be written as

$$K'_\alpha \cdot d'_\alpha = \bar{f}'_\alpha + f'_\alpha \qquad (1)$$

where $K'_\alpha = \int_{\Omega_\alpha^e} B'^{T}_\alpha \cdot D_\alpha \cdot B'_\alpha d\Omega$ is the elemental stiffness matrix of mathematical element α, $\bar{f}'_\alpha = \int_{\Gamma_{F\alpha}} N'^{T}_\alpha \cdot F_\alpha d\Gamma$ are the nodal forces from the boundary tractions and $f'_\alpha = \int_{\Gamma_{coh\alpha}} N'^{T}_\alpha \cdot t_\alpha d\Gamma$ are the nodal forces from the internal tractions due to the discontinuity. D_α is the material stiffness matrix. The prime at the upper right of a variable indicates that the variable is different from that of a standard element (SE). For example, shape functions of a ME (N'_α) are different from shape functions of a SE (N_α) because the ME has a different geometry with its corresponding physical domain. All the shape functions of ME strictly satisfy all the required properties for standard FE shape functions. There exists a mapping matrix which correlates the shape functions of a ME to the corresponding SE. The details of the mapping matrix are given in Ling's work [16].

Note that the stiffness integration within a mathematical element is performed on the active material domain, rather than on the entire elemental domain. The procedure of stiffness integration for ME is illustrated in *Figure 4*.

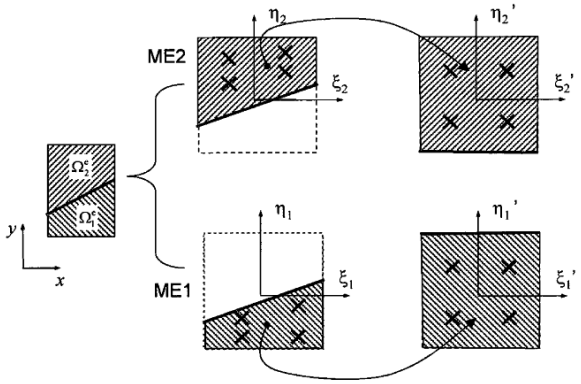

Figure 4 The sub-domain integration scheme[17]

First, the two MEs employed to describe the discontinuous displacement fields in the two physical domains are mapped into their corresponding isoparametric spaces, $\xi_1 - \eta_1$ and $\xi_2 - \eta_2$. Secondly, the physical domain in each ME is mapped into another isoparametric space $\xi'_1 - \eta'_1$ and $\xi'_2 - \eta'_2$, respectively to carry out the stiffness integration. In this way, the stiffness matrix for an ME can be concisely written as

$$K_\alpha = \int_{-1}^{1}\int_{-1}^{1} B'^{T}_\alpha \cdot D_\alpha \cdot B'_\alpha \cdot J_\alpha \cdot J'_\alpha d\xi d\eta \qquad (2)$$

where J_α is the Jacobian matrix that relates the actual area of a mathematical element and its area in isoparametric space; and J'_α is the Jacobian matrix that relates the area of a physical domain (shaded area) in a mathematical element to its area in isoparametric space.

3.2 Numerical implementation

A special purpose A-FEM program is implemented in Matlab®. Due to the use of interface elements and the internal tractions caused by discontinuities, the modified Newton-Raphson iteration method is implemented to solve the nonlinear equilibrium equations. Currently the program has two-dimensional capability.

4 Numerical verification

A few numerical studies were conducted to verify the A-FEM implementation. Two representative examples are shown below.

4.1 Crack propagation in a double cantilever beam (DCB)

This standard case of a propagating crack in a double cantilever beam (DCB) is used by Ling et al. [16] to demonstrate the ability of A-FEM to model long propagating cracks. This example is employed here to validate the prediction of crack length (*Figure 5*). This is a typical mode-I failure. Plane stress conditions were imposed. Geometry and cohesive parameters for fracture were identical to Ling's work [12].

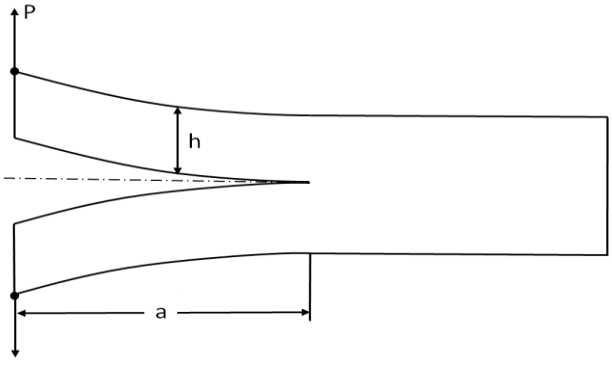

Figure 5 Double cantilever beam (DCB)

The analytical solution (Eq. 3) chosen for comparison is based on classical beam bending theory with transverse shear correction, which is known as modified DCB [28].

$$P = \sqrt{\frac{Eh\Gamma_I}{12}}\left[0.677 + \frac{a}{h}\right]^{-1} \qquad (3)$$

where P is the reaction force, E is the Young's modulus, Γ_I is the mode I fracture toughness, a is the crack length and h is the half height of the beam.

The results show good agreement between the numerical prediction and analytical solution (*Figure 6*).

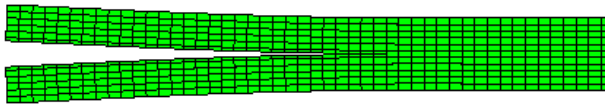

(a)

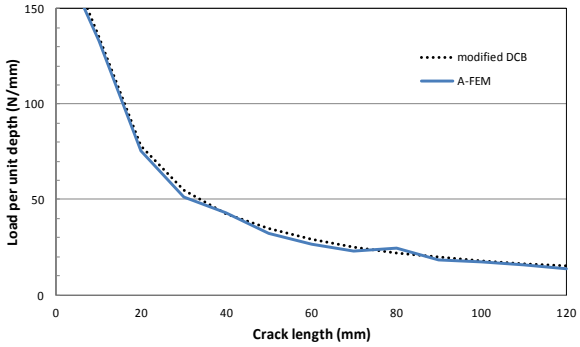

(b)

Figure 6 (a) A deformed DCB with a propagating crack; (b) numerically predicted fracture load versus crack length curve compared to an analytical solution (modified DCB)

4.2 Crack propagation in a beam under three-point bending

A simply supported beam is loaded symmetrically by means of an imposed displacement at the centre of the beam on the top edge (*Figure 7*). This example is employed to validate the prediction of crack propagation direction. Maximum principal stress criterion is used to determine the direction of crack growth. Since the tip of the crack is not located at a point where the stresses are known accurately (such as conventional Gauss points), the non-local stresses at the crack tip is calculated and used to find the principal directions. The details of the geometry and cohesive parameters for fracture were taken from Well's work [29]. An eccentric crack initiates at the bottom edge of the beam. The crack is expected to propagate in a curved path towards the centre at the top of the beam [26, 29]. Different crack initiation locations are tested; they all display the expected curved paths of the crack.

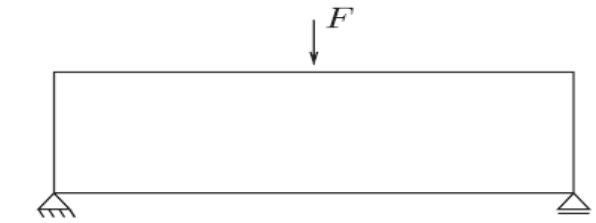

Figure 7 Three-point bending beam

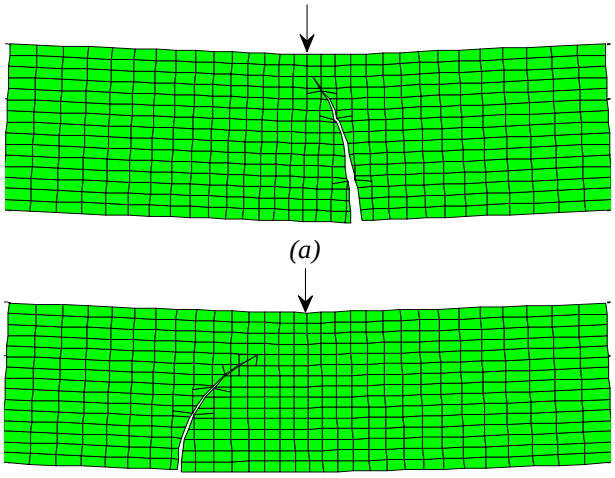

(a)

(b)

Figure 8 Propagation of the crack from eccentric locations

5 Aircraft coating studies

TiO_2 filler particles in the topcoat can cause polymer degradation reactions at the filler surface in the presence of UV, water and oxygen, so interfacial adhesion weakens with time. The program is applied to study the propagation of single cracks in coating systems with the aim to investigate the influence of the cohesive strength on crack behavior at material interfaces. Two representative volume elements (RVE) are extracted from the damage zone. Model A involves PU matrix and a few filler particles. Crack behavior at the interface between matrix and fillers will be observed. Model B involves both topcoat and primer. The topcoat is homogenized and fillers are not included in Model B. Crack behavior at the interface between topcoat and primer will be observed. In both models the crack initiates from the edge of topcoat and propagates under displacement controlled tensile loads. The strain level of the loads is set to 17%, which is taken from Tiong & Clark's work [30] in which they investigate the critical strain performance in aircraft coating systems. Plane strain condition is assumed. The CZM for interface elements is assumed to have a bilinear form which is based on the model proposed by Alfano and Crisfield [31]. The Cohesive parameters used in these initial studies reflect two extreme conditions of weak and strong bonds. The real cohesive zone model needs to be obtained through further experiments and correlation studies. Strain at break (ε_b) value is used in the program as fracture criterion. The results are stated as follows.

5.1 Model A

Material parameters of PU matrix are set to E = 150MPa and ν = 0.48; parameters of fillers are set to E = 280GPa and ν = 0.28. Two cases are tested. Case 1 has small cohesive strength (15MPa) (*Figure 9 a*). Case 2 has a bigger cohesive strength (3000MPa) (*Figure 9 b*).

Result of case 1 shows that delamination appears at filler boundaries before crack starts due to the weak cohesive forces (*Figure 10*). Note that, the small lines between matrix and filler elements represent interface elements. When the interface elements are working, it means that the clearance is a cohesive zone but not a crack. With the crack growth in PU matrix, it interacts with delamination cracks to form a major crack in topcoat (*Figure 11*).

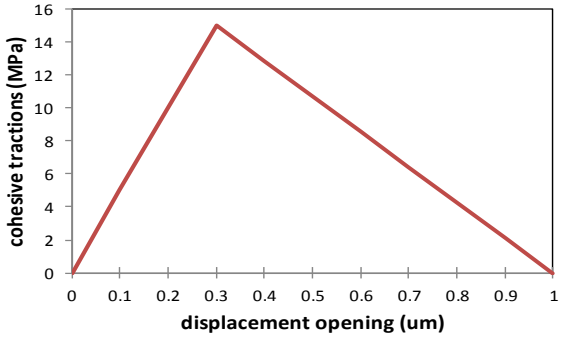

(a)

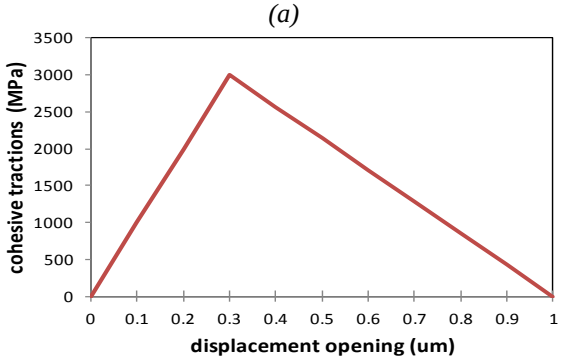

(b)

Figure 9 Cohesive constitutive law for Model A (a) Case 1 (b) Case 2

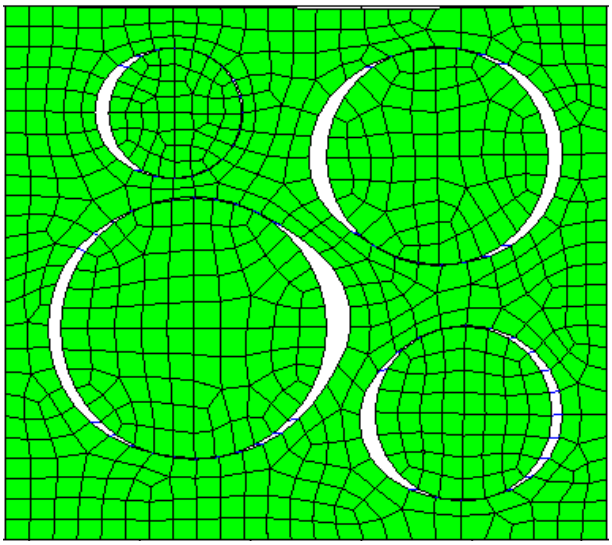

Figure 10 Case 1-- delamination before crack initiation

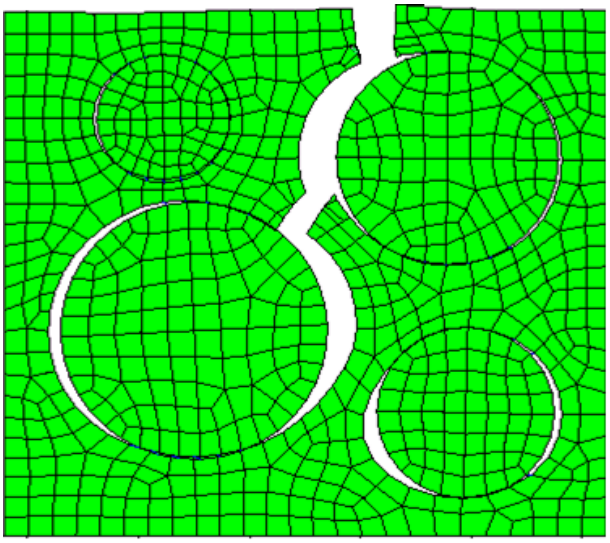

Figure 11 Case 1 -- a major crack forms

Result of case 2 shows that there is no delamination between matrix and particles before crack initiation (*Figure 12*). When crack grows and reaches the filler, it will stop at the interface and there is no further propagation. Then another crack may initiate from material interface. But when it reaches filler particle, it will stop as well (*Figure 13*).

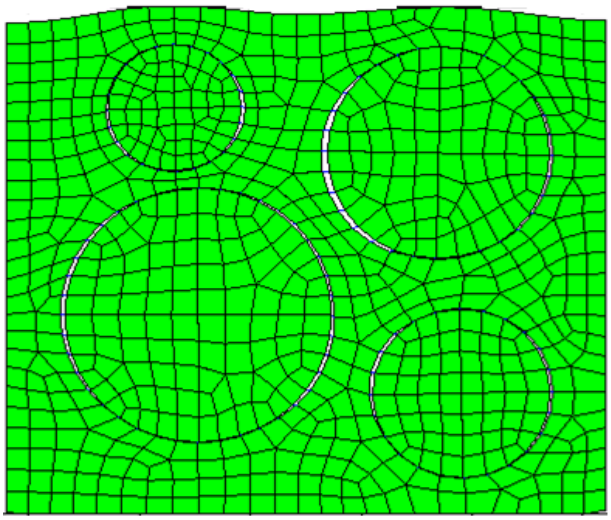

Figure 12 Case 2 -- deformation before crack initiation

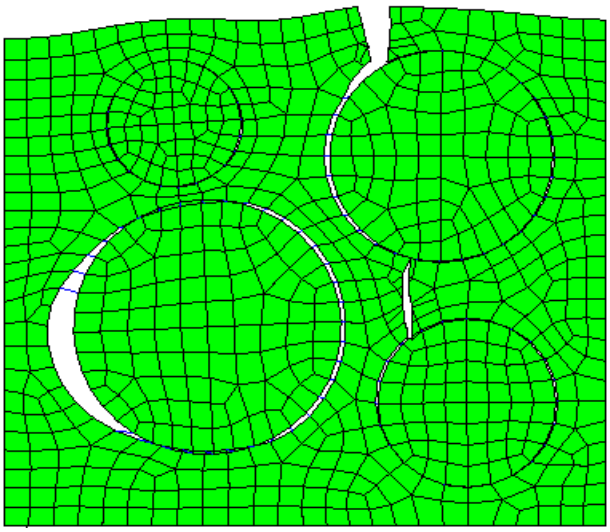

Figure 13 Case 2 -- Crack rests at material interface

Comparison of case 1 and case 2 points out that strong cohesive forces will be beneficial to stopping crack propagation in polymer matrix.

5.2 Model B

The material parameters of homogenized topcoat are set to E = 210MPa and ν = 0.49; parameters of epoxy primer are E = 1GPa and ν = 0.42. Two cases are tested. Case 1 has small cohesive strength (25MPa) (*Figure 14 a*). Case 2 has bigger cohesive strength (200MPa) (*Figure 14 b*).

When the crack arrives at the interface between topcoat and primer, the result of case 1 is delamination at the interface. At this instant, the maximum first principle strain at the interface of primer side is 19.2%, which means

that the crack will go into primer if ε_b is lower than 19.2% (*Figure 15*). The result of case 2 doesn't show delamination at the interface (*Figure 16*); the maximum strain level at interface is 22.5%, which is higher than that of case 1. Determination of the strain level at interface is important because it will affect the crack behavior – either halts at the interface or goes into primer. If the crack halts at the interface, it will help to prolong coating's life. Through comparing case 1 and case 2, we can appreciate that case 2 requires higher ε_b value to stop the crack to grow into primer, or case 1 is easier to stop the crack growing across the material interface. This conclusion can be explained considering the energy required to form new fracture surfaces. In case 1 part of the available fracture energy is consumed by the creation of the delamination at the interface.

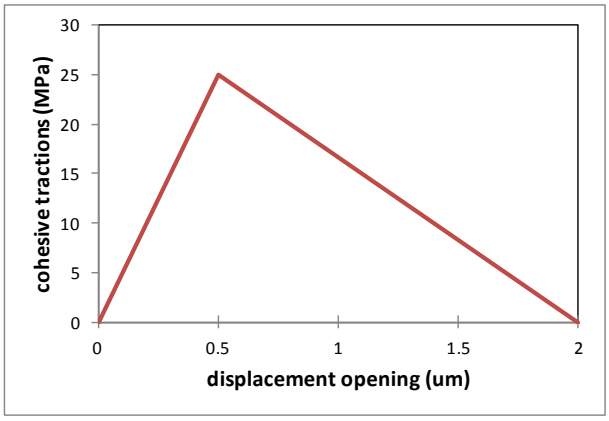

(a)

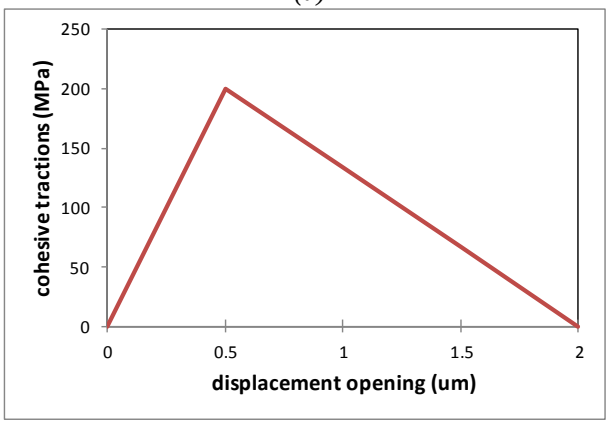

(b)

Figure 14 Cohesive constitutive law for model B (a) Case 1 (b) Case 2

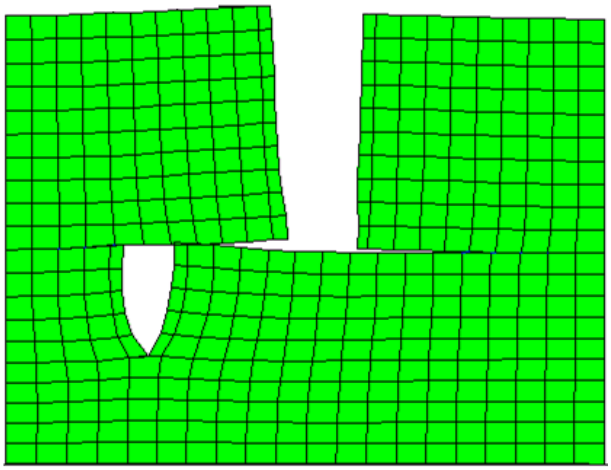

Figure 15 Case 1-- crack propagation from topcoat to primer with delamination at interface

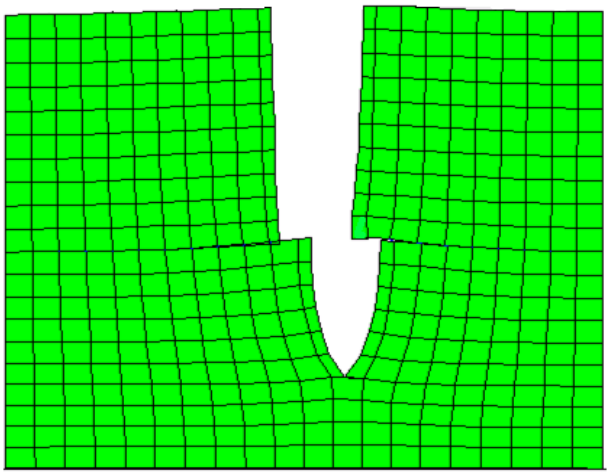

Figure 16 Case 2 -- crack propagation from topcoat to primer without delamination at interface

6 Conclusions

A special-purposed program is developed by combining both CZM and A-FEM methodology to investigate crack behavior during aircraft coating degradation. Numerical validation confirmed correct performance of the tool.

The tool has been applied for single crack studies in aircraft coating systems. The results show that strong cohesive tractions between PU matrix and filler particles are beneficial to stopping crack growth in the matrix; however, weak cohesive tractions would help to stop crack growth across the material interface between topcoat and primer because part of fracture energy is released through delamination at the interface.

The new simulation tool will be used in future studies to investigate the influence of: i) cohesive constitutive laws of the PU matrix materials on crack behavior; ii) filler size and shape on cohesive tractions; and iii) different loading conditions. In addition, experimental validation is currently in progress.

The ultimate goal of the project is to investigate how aging processes of aircraft coating systems, e.g. embrittlement of topcoat and primer, affect the propagation of microcracks. The numerical models will show when crack arrives at material interfaces, if delamination occurs at the topcoat-primer interface, or cracking of the primer is the dominant failure mechanism.

References

[1] D. L. Simpson and C. L. Brooks, "Tailoring the structural integrity process to meet the challenges of aging aircraft," *International Journal of Fatigue,* vol. 21, pp. 1-14, 1999.

[2] G. Clark, "Corrosion and the management of Structural Integrity," in *Structural Integrity for the Next Millennium*, J. L. Rudd, Ed., ed: EMAS, Warley, 1999.

[3] L. M. Farrier and S. L. Szaruga, "Sample preparation and characterization of artificially aged aircraft coatings for microstructural analysis," *Materials Characterization,* vol. 55, pp. 179-189, 2005.

[4] R. W. Hertzberg, *Deformation and fracture mechanics of engineering materials*: J. Wiley & Sons, 1996.

[5] J. R. Rice, "A path independent integral and the approximate analysis of strain concentration by notches and cracks," *J. Appl. Mech.,* vol. 35, 1968.

[6] D. S. Dugdale, "Yielding of steel sheets containing slits," *J. Mech. Phys. Solids,* vol. 8, pp. 100-104, 1960.

[7] G. I. Barenblatt, "The mathematical theory of equilibrium cracks in brittle fracture," *Advances in Applied Mechanics,* vol. 7, pp. 55-129, 1962.

[8] A. Hillerborg, *et al.*, "Analysisi of crack formation and crack growth in concrete by means of fracture mechanics and finite elements," *Cement and Concrete Research,* vol. 6, pp. 773-782, 1976.

[9] T. Belytschko and T. Black, "Elastic crack growth in finite elements with minimal remeshing," *International Journal for Numerical Methods in Engineering,* vol. 45, pp. 601-620, 1999.

[10] T. Belytschko, *et al.*, "Arbitrary discontinuities in finite elements," *International Journal for Numerical Methods in Engineering,* vol. 50, pp. 993-1013, 2001.

[11] J. Dolbow, *et al.*, "An extended finite element method for modeling crack growth with frictional contact," *Computer Methods in Applied Mechanics and Engineering,* vol. 190, pp. 6825-6846, 2001.

[12] N. Moës and T. Belytschko, "Extended finite element method for cohesive crack growth," *Engineering Fracture Mechanics,* vol. 69, pp. 813-833, 2002.

[13] Q. Z. Xiao and B. L. Karihaloo, "Implementation of hybrid crack element on a general finite element mesh and in combination with XFEM," *Computer Methods in Applied Mechanics and Engineering,* vol. 196, pp. 1864-1873, 2007.

[14] D. B. P. Huynh and T. Belytschko, "The extended finite element method for fracture in composite materials," *International Journal for Numerical Methods in Engineering,* vol. 77, pp. 214-239, 2009.

[15] B. Cox and Q. D. Yang, "In quest of virtual tests for structural composites," *Science,* vol. 314, pp. 1102-1107, 2006.

[16] D. Ling, *et al.*, "An augmented finite element method for modeling arbitrary discontinuities in composite materials," *Int J Fract,* vol. 156, pp. 53-73, 2009.

[17] Z. Zhou, "Multiple-scale numerical analysis of composites based on augmented finite element method," Ph.D. Dissertation, University of Miami, 2010.

[18] A. Hansbo and P. Hansbo, "An unfitted finite element method, based on Nitsche's method, for elliptic interface problems," *Computer Methods in Applied Mechanics and Engineering,* vol. 191, pp. 5537-5552, 2002.

[19] A. Hansbo and P. Hansbo, "A finite element method for the simulation of strong and weak discontinuities in solid mechanics," *Computer Methods in Applied Mechanics and Engineering,* vol. 193, pp. 3523-3540, 2004.

[20] J. H. Song, *et al.*, "A method for dynamic crack and shear band propagation with phantom nodes," *International Journal for Numerical Methods in Engineering,* vol. 67, pp. 868-893, Aug 8 2006.

[21] F. P. van der Meer and L. J. Sluys, "A phantom node formulation with mixed mode cohesive law for splitting in laminates," *International Journal of Fracture,* vol. 158, pp. 107-124, Aug 2009.

[22] T. Rabczuk, *et al.*, "A new crack tip element for the phantom-node method with arbitrary cohesive cracks," *International Journal for Numerical Methods in Engineering,* vol. 75, pp. 577-599, 2008.

[23] P. M. A. Areias and T. Belytschko, "A comment on the article "A finite element method for simulation of strong and weak discontinuities in solid mechanics" By A. Hansbo and P. Hansbo [Comput. methods Appl. Mech. Engrg. 193 (2004) 3523-3540]," *Computer Methods in Applied Mechanics and Engineering,* vol. 195, pp. 1275-1276, 2006.

[24] R. Jäger, *et al.*, "Modeling three-dimensional crack propagation-A comparison of crack path tracking strategies," *International Journal for Numerical*

Methods in Engineering, vol. 76, pp. 1328-1352, Nov 26 2008.

[25] P. Jäger, *et al.*, "On local tracking algorithms for the simulation of three-dimensional discontinuities," *Computational Mechanics*, vol. 42, pp. 395-406, 2008.

[26] J. Mergheim, *et al.*, "A finite element method for the computational modelling of cohesive cracks," *International Journal for Numerical Methods in Engineering*, vol. 63, pp. 276-289, 2005.

[27] J. Mergheim, *et al.*, "Towards the algorithmic treatment of 3D strong discontinuities," *Communications in Numerical Methods in Engineering*, vol. 23, pp. 97-108, 2007.

[28] M. N. Cavalli and M. D. Thouless, "The effect of damage nucleation on the toughness of an adhesive joint," *The Journal of Adhesion*, vol. 76, pp. 75-92, 2001.

[29] G. N. Wells and L. J. Sluys, "A new method for modelling cohesive cracks using finite elements," *International Journal for Numerical Methods in Engineering*, vol. 50, pp. 2667-2682, 2001.

[30] U. H. Tiong and G. Clark, "Critical strain performance of coating systems at aircraft joints," presented at the 27th International Congress of the Aeronautical Sciences, Nice, France, 2010.

[31] G. Alfano and M. A. Crisfield, "Finite element interface models for the delamination analysis of laminated composites: mechanical and computational issues," *International Journal for Numerial Methods in Engineering*, vol. 50, pp. 1701-1736, 2001.

Acknowledgement

The authors would like to acknowledge the financial support from the Defence Materials Technology Centre (DMTC) and the Queensland Centre for Advanced Materials Processing and Manufacturing (AMPAM). The DMTC was established and is supported under the Australian Government's Defence Future Capability Technology Centre's Program.

Copyright Statement